

Study on chemical state of Sn in ITO by Mössbauer spectrometry

N. Yamada,^{a)} Y. Shigesato,^{a)} I. Yasui,^{a)} H. Li,^{b)} Y. Ujihira,^{b)} K. Nomura^{c)}

a) Institute of Industrial Science, University of Tokyo, Minato-ku, Tokyo 106, Japan

b) Research Center of Advanced Science and Technology, University of Tokyo, Meguro-ku, Tokyo 153, Japan

c) Faculty of Engineering, University of Tokyo, Bunkyo-ku, Tokyo 113, Japan

ABSTRACT

^{119}Sn Mössbauer studies on Sn-doped In_2O_3 (ITO for Indium Tin Oxide) powders with different Sn doping concentrations were carried out. Transmission Mössbauer spectra exhibited that all Sn atoms in ITO were in 4+ state. Deconvolution analysis of the spectra made it possible to distinguish between electrically active Sn and inactive dopants, and hence to estimate the amounts of them in the material. Steady increase in the electrically inactive Sn, such as $\text{Sn}'_2\text{O}_i$ and $(\text{Sn}_2\text{O}_4)^x$, was clearly observed with increasing Sn doping concentration in the powders. Carrier densities were estimated for the each sample, taking account of the concentration of the active Sn dopants, which was in good agreement with the measured values for splayed ITO films.

1. INTRODUCTION

Tin-doped In_2O_3 (ITO) is an n-type, highly degenerated, wide-gap semiconductor, which shows low resistivity ($\sim 10^{-4}\Omega\text{cm}$) and high transmittance (above 80%) in visible region. ITO thin films have been applied to optoelectronic devices, such as transparent electrodes of flat panel displays and solar cells. With recent demands for large size and high quality flat panel displays, ITO films are required to have extremely low resistivity less than $10^{-4}\Omega\text{cm}$. The electrical and optical properties of the ITO thin films had been extensively investigated^{1,2}. Both of these properties are intimately associated with microstructure³⁻⁷ and lattice defects^{8,9} of the films.

Chemical state of Sn in this material is one of the most important key factors to achieve the lower resistivity, since substitutional four-valent Sn on In^{3+} site (Sn'_{In}) is one of the dominant donor sites. A phenomenon that doping efficiency decreases with increasing Sn doping concentration at about 5-10 atomic% has been reported¹, which was considered to originate in the presence of electrically neutralized dopants at higher doping concentrations. There were a few reports on the

chemical states of Sn in ITO¹⁰⁻¹⁵, however, the mechanism of donor compensation effect has been cleared. Frank et. al. proposed⁸ two models of neutralized Sn dopants, such as $\text{Sn}'_2\text{O}_i$ and $(\text{Sn}_2\text{O}_4)^x$, which were comprised of interstitial oxygen anion (O_i'') and substitutional tin (Sn'_{In}) on indium site. Their models could explain the dependence of the carrier density on the Sn doping concentration, however no evidence for existence of such defects has been reported.

Mössbauer spectroscopy is one of the powerful technique for investigations on lattice defects, since the spectra are sensitive to symmetry of coordination around the Mössbauer atoms. In order to clarify the presence of the neutralized Sn and doping mechanism, ^{119}Sn Mössbauer studies on Sn in ITO powders with different Sn doping concentrations were performed in view of crystal structure.

2. EXPERIMENTALS

ITO Powders were prepared by sintering the mixtures of In_2O_3 and SnO_2 powders with Sn concentrations of 0.5, 2.5, 5.0, 7.0, and 10at% at

1500 °C for several hours under atmospheric condition.

Transmission Mössbauer spectra of the ITO powders were obtained using a NaI(Tl) scintillation counter. 1mCi Ba^{119m}SnO₃ was used as γ -ray source. The isomer shifts were referred to SnO₂ at room temperature. The velocity was calibrated using a 10mCi ⁵⁷Co(Rh) source and enriched ⁵⁷Fe foil as an absorber. The spectra were fitted as a sum of three doublets (sub-spectra) composed of Lorentzian curves by the non-linear least-squares program. In order to assign the sub-spectrum to Sn in the different chemical state, electric field gradient and asymmetric parameter at each Sn site was calculated with point charge approximation.

3. EXPERIMENTAL RESULTS

The obtained spectra were fitted with the three doublets, assuming that each sub-spectrum was Lorentzian. The goodness of the fitting (χ^2) was about 1.0, which was considered to be very satisfactory. The sub-spectra were named COMP.1, COMP.2, and COMP.3, respectively, in order of magnitude of quadrupole splitting. Different quadrupole splitting values imply that Sn is located at the different sites. The isomer shift (IS) relative to SnO₂, quadrupole splitting (QS), and relative area of each spectrum are listed in Table 1. At lower Sn concentration (<5.0at%), each fitting spectrum consists of two sub-spectra. On the other hand, the fitting spectra consist of three sub-spectra at higher Sn concentration (\geq 5.0at%). The IS values of all components indicated that all Sn atoms in the ITO powders were in 4+ states. Neither Sn²⁺ nor metallic Sn were detected in the samples. The QS values of all components became larger with increasing doping concentrations, which should be the results of increasing local disorder around the dopant Sn. The relative areas of COMP.2, and COMP.3

showed steady increase with increasing Sn concentration.

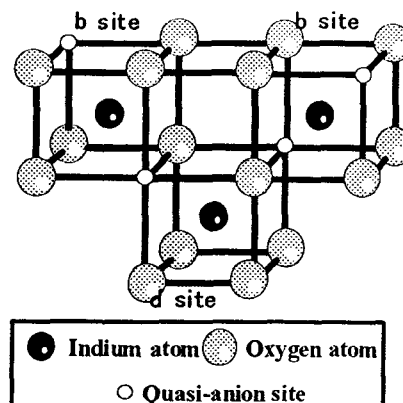


Fig. 1 The crystal structure of In₂O₃ host lattice

4 DISCUSSIONS

4.1 Crystal Structure of ITO distorted

Before discussing the relationship between defect models and Mössbauer results, a short description of crystal structure of the ITO is required. X-ray diffraction patterns of the all ITO powders showed clear In₂O₃ cubic bixbyite structure without any SnO₂ peaks. There are two non-equivalent In atom sites in In₂O₃ crystal. In the unit cell, 8/32 of indium atoms occupy the center of trigonally distorted oxygen octahedron (b site) and the remaining 24/32 located at the center of more distorted octahedra (d site)¹⁶. Both of the Indium sites are surrounded by six oxygen atoms and adjacent to quasi-anion sites. A part of In₂O₃ lattice is shown in Fig. 1.

4.2 Defect Models in ITO

The doping mechanism had been investigated by several author in terms of interstitial Sn atoms¹⁷ or Sn₃O₄-like phase¹⁰.

Parent et. al.^{11,12}, by means of EXAFS, reported that interstitial Sn atoms did not exist in view of radial structure functions. And a detail XPS

Table1. Obtained Mossbauer parameters and relative areas

Sn conc. (at%)	COMP.1			COMP.2			COMP.3			χ spur
	IS (mm/sec)	QS (mm/sec)	area (%)	IS (mm/sec)	QS (mm/sec)	area (%)	IS (mm/sec)	QS (mm/sec)	area (%)	
0.5	0.17	0.5	80	0.23	0.47	20	-	-	0	1.038
2.5	0.17	0.65	68	0.22	0.61	32	-	-	0	1.003
5.0	0.15	0.7	62	0.16	0.68	36	0.16	0.21	2	1.004
7.0	0.12	0.75	36	0.15	0.67	61	0.13	0.21	3	1.118
10	0.11	0.84	26	0.15	0.78	69	0.12	0.21	5	1.004

analysis of Sn 3d spectra¹³ suggested no evidence for existence of Sn₃O₄-like phase.

The most reliable defect models were proposed by Frank et. al.⁸, which were summarized as follows.

Sn_b, Sn_d:

Sn⁴⁺ on In³⁺ (b or d) site ; effective dopant

Sn₂O²⁻:

O²⁻ on interstitial quasi-anion site, loosely bound to two Sn⁴⁺ which don't occupy nearest neighbor In³⁺ positions ; neutralized dopant.

(Sn₂O₄)^x:

Strongly bound complex, similar to Ca₂F₄, composed of two nearest neighbor Sn⁴⁺, surrounded by three nearest neighbor O²⁻ on regular anion sites, and one interstitial O²⁻ on quasi-anion site in the In₂O₃ lattice. ; neutralized dopant.

According to these defect models, there are four kinds of Sn atoms in the ITO.

Each Sn species should be under different electric field gradient resulting in different QS in the Mössbauer spectrum. Point charge calculations of electric field gradients and asymmetric parameters were performed in order for the assignment of individual sub-spectrum to Sn atoms on the different site, since magnitude of the QS is nearly proportioned to the electric field gradient. The calculated electric field gradients (EFG) and asymmetric parameters (η) are listed in Table 2. Based on the results in Table 1 and Table 2, it is considered that COMP.1 could be assigned to Sn_b, COMP.2 could be assigned to Sn_d or Sn₂O²⁻, and COMP.3 could be assigned to (Sn₂O₄)^x. The relative area of COMP.2 increased abruptly at higher (>5at%) Sn doping concentration, where doping efficiency started to decrease¹ with increasing Sn concentration. This suggest that the amount of Sn₂O²⁻ (neutralized Sn) is considered to have increased at higher Sn doping concentration around 5at%.

Table 2
The calculated values of EFG and asymmetric parameter (η) at different locations of Sn atoms

	EFG (×10 ¹⁷ V/cm ²)	η
Sn _b	12.1	0.0
Sn _d	6.1	1.0
Sn ₂ O ²⁻	6.1	0.0
(Sn ₂ O ₄) ^x	0.0	-

Since the relative area of each component sub-spectrum implies amount of Sn species located at the corresponding chemical state, the concentrations of each Sn defect could be estimated using the relative areas of sub-spectra.

The dependence of the each defect concentration in the powder ITO on the Sn doping concentration is given in Fig.2. The concentrations of electrically active dopants, such as Sn_b, and Sn_d, linearly increased with increasing Sn concentration at lower doping concentration (region 1 in the Fig.2) and saturated at higher doping concentration around 5at% (region 2 in the Fig.2). The concentration of Sn_b was higher than that of Sn_d, which should be caused by the more similar configuration of oxygen atoms around the b sites to the one around Sn atom in the SnO₂ rutil crystal structure. The amounts of neutralized dopants, such as interstitial defect [Sn₂O²⁻] and neutral complex [(Sn₂O₄)^x] appeared and linearly increased with increasing Sn concentration at the higher Sn concentration. These neutral defects cannot donate the free electron and exist as the neutral impurity scattering centers in the ITO, which cause the decreasing in the doping efficiency and hence the mobility of free carriers.

It was reported that the host network was distorted with Sn doping, which was consistent with steady increase in QS values with increasing Sn concentration because the distortion of the host

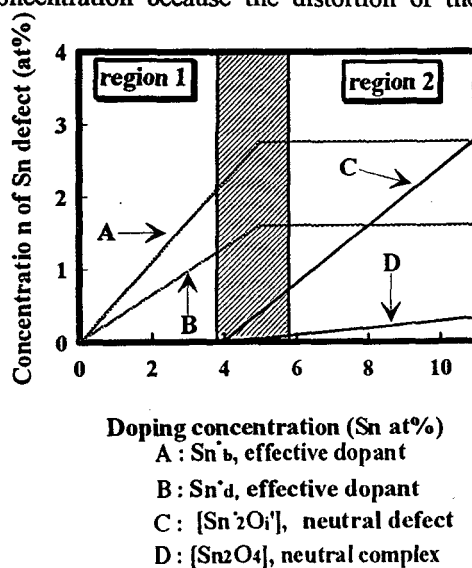


Fig. 2
Dependence of defect concentration on doping concentration

network should induce the increase in of host network induce the increase of the electric field gradient and the asymmetric parameter around the dopant Sn atoms.

4.3 Estimation of Carrier Density

Carrier densities of the samples were estimated on the basis of Fig.2, assuming that the only Sn_b or Sn_d donate one electron. Comparison was made between the estimated carrier densities for powder samples from the Mössbauer analysis and the measured values for films deposited using spray pyrolysis technique, because the spray pyrolysis was not so non-equilibrium technique compared with sputtering or another PVD technique. In Fig.3, both of the values were plotted as a function of the doping concentrations. In this figure, the estimated values were in good agreement with the measured values for the films, indicating that the analysis and the assignments should be reasonable.

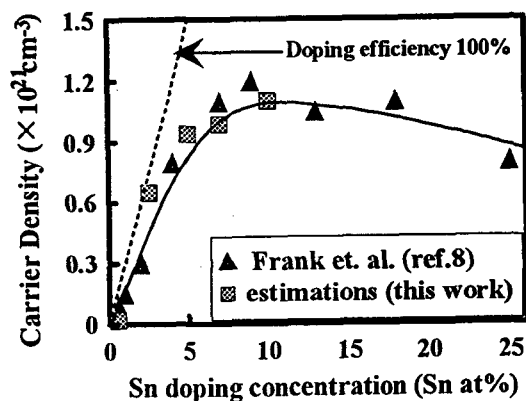


Fig. 3 Comparison between the estimated and measured carrier density

5. CONCLUSIONS

In this study, the Mössbauer results could be successfully related to the electrical properties of ITO films.

The deconvolution analysis of ^{119}Sn Mössbauer spectra of the powder ITO made it possible to distinguish the electrically active and inactive Sn dopants. The steady increase in neutralized Sn dopants, such as Sn_2O_3 and $(\text{Sn}_2\text{O}_4)^x$, were clearly observed with increasing Sn doping concentration

in the powders, which demonstrated the low doping efficiency with highly doped ITO.

The estimated carrier densities of the powders from the Mössbauer results were in good agreement with that of ITO film deposited by spray pyrolysis.

These two results suggested that both (i) increasing the electrically active Sn substituted to In atoms (Sn_b or Sn_d) and (ii) decreasing the electrically neutralized Sn which are exist only as neutral scattering centers (Sn_2O_3 or $(\text{Sn}_2\text{O}_4)^x$) should be important to obtain ITO films with the extremely low resistivity.

REFERENCES

1. H. Köstlin, R. Jost, and W. Rems, *Phys. Stat. Sol. (a)* **29**, 87 (1975).
2. I. Hamberg and C. G. Granqvist, *J. Appl. Phys.* **60**, R123 (1986).
3. Y. Shigesato, D. C. Paine and T. E Haynes, *J. Appl. Phys.* **8**, 73 (1993).
4. Y. Shigesato, D. C. Paine and T. E Haynes, *Jpn. J. Appl. Phys.* **32**, 9B (1993).
5. C. H. Yi, I. Yasui, Y. Shigesato, *Jpn. J. Appl. Phys.* **34**, 1638 (1995).
6. C. H. Yi, I. Yasui, Y. Shigesato, *Jpn. J. Appl. Phys.* **34**, L244 (1995).
7. Y. Shigesato, D. C. Paine, *Thin Solid Films*, **238**, 44 (1994).
8. G. Frank and H. Köstlin, *Appl. Phys.* **A27**, 197 (1982).
9. T. E. Haynes and Y. Shigesato, *J. Appl. Phys.* **77**, 2572 (1995).
10. J. C. C. Fan and J. B. Goodenough, *J. Appl. Phys.* **48**, 3524 (1977).
11. P. Parent, H. Dexpert, G. Tourillon and J. M. Grimal, *J. Electrochem. Soc.* **139**, 276, (1992).
12. P. Parent, H. Dexpert, G. Tourillon and J. M. Grimal, *J. Electrochem. Soc.* **139**, 282, (1992).
13. A. J. Nelson and H. Aharoni, *J. Vac. Sci. Technol.* **A5**(2), 231 (1987).
14. K. Nomura, Y. Ujihira, S. Tanaka and K. Matsumoto, *Hyp. Int.* **42**, 1207 (1988).
15. R. G. Geere and P. H. Gaskell, *Rivista della Staz. Sper. Vetro* n. 6 153 (1990).
16. M. Marezio, *Acta Cryst.* **20**, 723 (1966).
17. Y. Shigesato, S. Takaki and T. Haranoh, *Appl. Surface Sci.* **48/49**, 269 (1991).